The EMBO Journal (2009) 28, 405–416 | © 2009 European Molecular Biology Organization | All Rights Reserved 0261-4189/09
www.embojournal.org

THE EMBO JOURNAL

BLM helicase measures DNA unwound before switching strands and hRPA promotes unwinding reinitiation

Jaya G Yodh[1], Benjamin C Stevens[1], Radhakrishnan Kanagaraj[2], Pavel Janscak[2,3] and Taekjip Ha[1,4,*]

[1]Department of Physics, Center for the Physics of Living Cells, University of Illinois at Urbana-Champaign, Urbana, IL, USA; [2]Institute of Molecular Cancer Research, University of Zurich, Zurich, Switzerland; [3]Institute of Molecular Genetics AS CR, Prague, Czech Republic and [4]Howard Hughes Medical Institute, Urbana, IL, USA

Bloom syndrome (BS) is a rare genetic disorder characterized by genomic instability and a high predisposition to cancer. The gene defective in BS, *BLM*, encodes a member of the RecQ family of 3′–5′ DNA helicases, and is proposed to function in recombinational repair during DNA replication. Here, we have utilized single-molecule fluorescence resonance energy transfer microscopy to examine the behaviour of BLM on forked DNA substrates. Strikingly, BLM unwound individual DNA molecules in a repetitive manner, unwinding a short length of duplex DNA followed by rapid reannealing and reinitiation of unwinding in several successions. Our results show that a monomeric BLM can 'measure' how many base pairs it has unwound, and once it has unwound a critical length, it reverses the unwinding reaction through strand switching and translocating on the opposing strand. Repetitive unwinding persisted even in the presence of hRPA, and interaction between wild-type BLM and hRPA was necessary for unwinding reinitiation on hRPA-coated DNA. The reported activities may facilitate BLM processing of stalled replication forks and illegitimately formed recombination intermediates.

The EMBO Journal (2009) **28,** 405–416. doi:10.1038/emboj.2008.298; Published online 22 January 2009
Subject Categories: genome stability & dynamics
Keywords: Bloom syndrome; FRET; helicase; hRPA; single molecule

Introduction

The human *BLM* gene is mutated in Bloom syndrome (BS), a rare autosomal recessive disorder characterized by genomic instability and clinical phenotypes, including a high predisposition to cancer of multiple types, infertility, and dwarfism (Bachrati and Hickson, 2003; Opresko *et al*, 2004). The genomic instability present in BS cells manifests as a high frequency of sister chromatid exchanges, hyper-recombination, and aberrant DNA replication phenotypes. The *BLM* gene product, BLM, is a member of the RecQ family of DNA helicases and catalyses single-stranded (ss) DNA-dependent ATP hydrolysis as well as ATP-dependent 3′–5′ unwinding of duplex DNA (Karow *et al*, 1997). A unique feature of BLM is its ability to unwind a variety of DNA structures that may arise as intermediates during replication and homologous recombination (HR) (Mohaghegh *et al*, 2001). BLM has been proposed to function in replication fork repair through multiple mechanisms, including unwinding non-canonical structures that cause fork stalling, preventing illegitimate recombination events during replication, and resetting forks stalled due to template strand lesions (Wu and Hickson, 2006; Bachrati and Hickson, 2008). BLM also has a regulatory role in HR, acting as both an antirecombinase and a promoter of recombination (Wu and Hickson, 2006; Hanada and Hickson, 2007).

Despite extensive characterization of BLM DNA unwinding substrate specificity, its mechanism of unwinding has not been clear. Thus far, studies have relied on gel electrophoresis-based oligonucleotide displacement assays that detect only completely unwound products (Bachrati and Hickson, 2006). To date, no partially unwound intermediates have been observed during BLM unwinding. Two other aspects that merit further study are the role of human replication protein A (hRPA) (Wold, 1997) and the oligomeric state of the BLM catalytic unit. *In vitro*, hRPA enhances the ability of BLM to unwind long duplex DNAs through direct hRPA–BLM interactions under multiple turnover conditions (Brosh *et al*, 2000; Doherty *et al*, 2005). The question if and how hRPA impacts unwinding on forked substrates with shorter duplex regions has not been investigated. Structural studies have shown that BLM assembles into a ring structure (Karow *et al*, 1999), and an oligomerization domain has been mapped to the N-terminal tail (Beresten *et al*, 1999). However, a $BLM^{642–1290}$ mutant lacking this oligomerization domain is sufficient for unwinding (Janscak *et al*, 2003), providing evidence for a monomeric catalytic unit.

We have utilized single-molecule fluorescence resonance energy transfer (smFRET) to shed light on the mechanism of BLM-catalysed DNA unwinding. Single-molecule analysis allows for detection of reaction intermediates and multiple pathways in real time that are difficult to measure in bulk solution (Perkins *et al*, 2004; Handa *et al*, 2005; Lee *et al*, 2006; Johnson *et al*, 2007; Lionnet *et al*, 2007; Sun *et al*, 2008). In previous investigations, the high spatio-temporal resolution provided by smFRET has been useful in elucidating DNA translocation and unwinding mechanisms of *Escherichia coli* Rep helicase and hepatitis C virus NS3 helicase (Ha *et al*, 2002; Myong *et al*, 2005, 2007).

Here, we report a previously unknown activity of BLM to unwind DNA repetitively. BLM unwinds a critical length of duplex DNA, which then reanneals rapidly, followed by more

*Corresponding author. Department of Physics, Center for the Physics of Living Cells, University of Illinois, 1110 W Green Street, Urbana, IL 61801, USA. Tel.: +1 217 265 0717; Fax: +1 217 244 7187; E-mail: tjha@illinois.edu

Received: 28 August 2008; accepted: 17 December 2008; published online: 22 January 2009

cycles of unwinding/reannealing that occur very regularly. This 'repetitive unwinding' behaviour was observed with both $BLM^{642-1290}$, a mutant encompassing the RecQ helicase core of BLM (core-BLM), and wild-type (WT) BLM. Our data support a model in which a monomeric BLM 'measures' the amount of DNA unwound before reversal of unwinding through strand switching. Repetitive unwinding persisted in the presence of hRPA, which produced a limited increase in unwinding processivity, and direct interaction between hRPA and WT-BLM was necessary for efficient reinitiation of unwinding on hRPA-coated DNA. Potential roles for BLM strand switching during unwinding of forked substrates in replication fork repair and prevention of illegitimate HR are discussed.

Results

Substrate for smFRET unwinding assay

To investigate the unwinding by BLM on single DNA molecules, we prepared fluorescently labelled forked substrates as described in Materials and methods. FK34 is a typical substrate (Figure 1A), which contains a 34-bp dsDNA with a 3′ T_{30} ss tail containing donor (Cy3) at the junction and a 5′ ss T_{24} tail containing acceptor (Cy5) that is 7 nucleotides (nt) away from the junction. The substrate is tethered to the PEG surface through a biotin at the end of the 5′ tail. Before unwinding, FRET between the two fluorophores is high due to close proximity and is expected to decrease during unwinding as they become separated (Ha *et al*, 2002; Myong *et al*, 2007). In addition, unwinding completion and release of the donor-labelled strand from the surface would result in abrupt disappearance of the total fluorescence signal. This substrate was designed with the following considerations: (1) the forked structure is preferred by BLM (Mohaghegh *et al*, 2001); (2) the 3′ tail (tracking strand) is untethered and thus more accessible to BLM; (3) the duplex faces away from the slide surface and is thus unconstrained; and (4) the dyes are spaced such that contact-induced quenching between Cy3 and Cy5 is minimized. In Supplementary Figure S1, we demonstrate that FK34 can be fully unwound by BLM at high concentrations using a native PAGE gel unwinding assay.

Single-molecule histograms under unwinding conditions

Histograms of FRET efficiencies for FK34 DNA show a high FRET value due to the proximity of the dyes (Figure 1B, black). The small population at a low FRET value is due to the donor-only DNA species. The addition of $BLM^{642-1290}$ (core-BLM) alone (10 nM) has a minimal effect on the FRET distribution (blue). Upon addition of core-BLM (10 nM) and ATP (20 μM), the DNA is partially unwound as indicated by a decrease in the population of high FRET species and a corresponding increase in mid-FRET species (red). Even over 5 min, we did not observe a significant decrease in the number of fluorescent spots. Therefore, full unwinding of a 34-bp duplex is rare under this condition.

Repetitive unwinding of DNA by core-BLM

Figure 1C displays representative single-molecule time traces during unwinding of FK34 catalysed by core-BLM. Unwinding is characterized by a gradual decrease in donor intensity (green, upper panel) with an accompanying

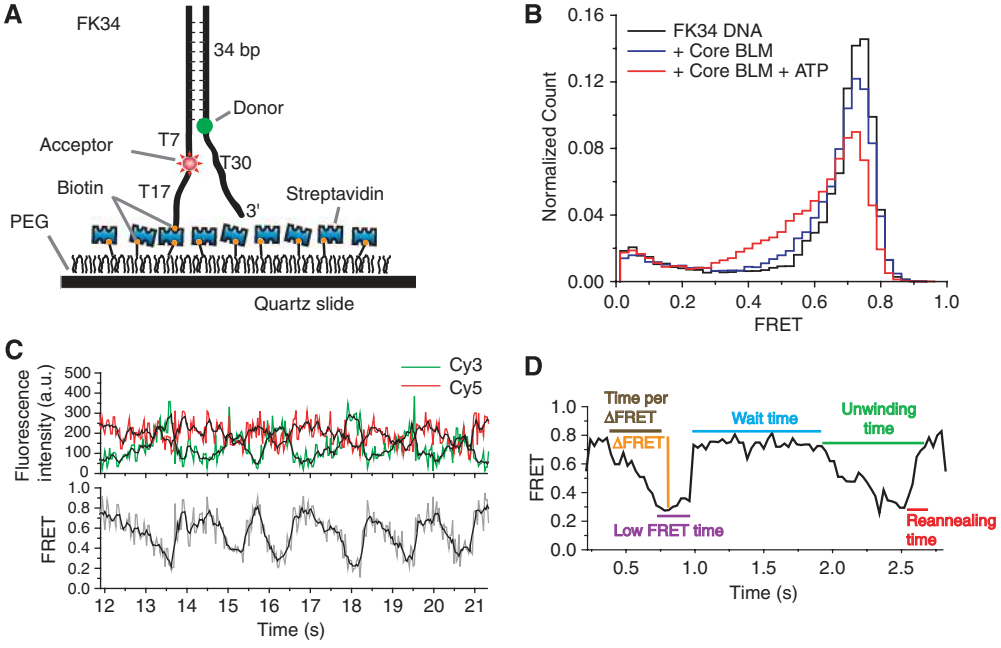

Figure 1 Repetitive unwinding by BLM revealed by smFRET. (**A**) Partial-duplex forked substrate, FK34, contains a 34 bp dsDNA with a 3′ T_{30} ss tail containing donor (Cy3, green) at the junction and a 5′ ss T_{24} tail containing acceptor (Cy5, red) 7 nt 5′ to the junction. The substrate is tethered to the PEG surface through 5′ biotin. (**B**) Single-molecule FRET histograms of FK34 DNA (black); + 10 nM core-BLM (blue), and + 10 nM core-BLM + 20 μM ATP (red). Histograms were normalized for the number of molecules. (**C**) Representative single-molecule time traces (30 ms integration time) of donor (green) and acceptor (red) fluorescence intensities (upper panel) and corresponding FRET (lower panel)). Raw time traces are shown in colour, whereas the three-point averaged traces are shown in black. (**D**) Schematic diagram of parameters to be quantitated from FRET time traces (refer to Results 'Characterizing each cycle of repetitive unwinding' for a detailed description).

Table I Oligonucleotide sequences for the preparation of DNA unwinding substrates

Substrate	Sequence
FK34	5′-**B**-T17-**iCy5**-T7-CAAGGCACTGGTAGAATTCGGCAGCGTGCTTCTC-3′ 5′-GAGAAGCACGCTGCCGAATTCTACCAGTGCCTTG-**1**-T30-3′
FK34-T60	5′-**B**-T17-**iCy5**-T7-CAAGGCACTGGTAGAATTCGGCAGCGTGCTTCTC-3′ 5′-GAGAAGCACGCTGCCGAATTCTACCAGTGCCTTG-**1**-T60-3′
FK34-GC	5′-**B**-T17-**iCy5**-T7-ATTGCGGGGCGGGCGGGGCGGCGGGCGCGGGCGG-3′ 5′-ATTGCGGGGCGGGCGGGGCGGCGGGCGCGGGCGG-**1**-T30-3′
FK50a	5′-**B**-T17-**iCy5**-T7-CAAGGCACTGGTAGAATTCGGCAGCGTGCTTCTCATGTCTCACATGTCCT-3′ 5′-AGGACATGTGAGACATGAGAAGCACGCTGCCGAATTCTACCAGTGCCTTG-**1**-T30-3′
FK50	5′-**B**-T4-**iCy5**-T4-GGCAAACATGTCCTAGCAAGGCACTGGTAGAATTCGGCAGCGTGCTTCTC-3′ 5′-GAGAAGCACGCTGCCGAATTCTACCAGTGCCTTGCTAGGACATGTTTGCC-**1**-T30-3′
NonFK50-3′-tether	5′-**Cy5**-GGCAAACATGTCCTAGCAAGGCACTGGTAGAATTCGGCAGCGTGCTTCTC-3′ 5′-GAGAAGCACGCTGCCGAATTCTACCAGTGCCTTGCTAGGACATGTTTGCC-**1**-T30-**B**-3′

FK, forked; NonFK, no fork; B, biotin; 1, amino modifier C6 dT (for labelling with Cy3); iCy5, phosphoramidite-backbone labelled Cy5; Cy5 refers to end-labelled position generated through phosphoramidite chemistry.

increase in acceptor intensity (red, upper panel) and a corresponding change from high to low FRET (lower panel). Interestingly, we observe 'repetitive unwinding' events on individual DNA molecules in which a certain length of DNA is unwound and then rapidly reannealed (marked by quick recovery of FRET) followed by reinitiation of unwinding in several successions. At 30-ms time resolution, we have observed repetitive unwinding on a single molecule for up to 60 s beyond which we are constrained by photobleaching. Repetitive unwinding required ATP hydrolysis and a 3′ ss tail because no unwinding was observed in the presence of ATPγS or using a partial duplex substrate with a tethered 5′ tail but lacking a 3′ tail (data not shown). WT-BLM also displays repetitive unwinding (see below).

The repetitive unwinding behaviour was also observed on other substrates with variations in several features relative to FK34 (Table I; Supplementary Figure S2 and data not shown), including duplex regions of varying length (18–50 bp) and sequences (52–92% GC); substrates in which either the duplex end, 5′ ss tail (8–40 nt), or 3′ ss tail (10–60 nt) is attached to the surface; forked structures as well as non-forked 3′-tailed DNA; and varying positions of Cy3 and Cy5 dyes on the ss tails relative to the junction. In particular, we rule out the possibility that FRET decrease is caused by BLM translocation on ssDNA tails instead of unwinding because (1) a 3′-tailed DNA with both dyes at the junction still showed repetitive FRET changes (Supplementary Figure S2F) and a similar substrate showed FRET decreases only during unwinding but not during ssDNA translocation by the Rep helicase (Ha *et al*, 2002) and (2) increasing GC content in the duplex region of otherwise identical DNA substrates lengthens both the *ΔFRET* and *Time per ΔFRET* (parameters described below, Supplementary Figure S3).

Characterizing each cycle of repetitive unwinding

Each unwinding event is characterized by three phases: (I) a phase during which FRET decreases due to unwinding, followed by (II) a time period during which FRET remains at a constant low value, followed by (III) a reannealing phase characterized by a rapid switch back to high FRET. To quantitatively describe repetitive unwinding, we measure several parameters (Figure 1D):

- *Unwinding Time*: Duration of the entire event including all three phases;
- Δ*FRET*: Drop in FRET during phase I;
- *Time per ΔFRET*: Duration of phase I during which FRET decreases;
- *Low FRET Time*: Duration of phase II;
- *Reannealing Time*: Duration of phase III; and
- *Wait Time*: The time period between events during which no unwinding takes place and FRET remains high.

Under our conditions, *Time per ΔFRET*, *Low FRET Time*, and *Reannealing Time* comprise approximately 60, 25, and 15%, respectively, of *Unwinding Time*. Supplementary Figure S4 displays two-dimensional density plots of hundreds of FK34 smFRET time traces simultaneously averaged over each phase of repetitive unwinding. From the *Wait Time* averaging, we obtained a standard deviation of 0.08, which is a measure of FRET noise level at the time resolution of 30 ms.

Less than 34 bp is unwound during repetitive unwinding

We can estimate how FRET values correlate with the number of base pairs unwound based on a study probing ssDNA conformational flexibility using FRET (Murphy *et al*, 2004) such that minimal and maximal separation of FK34 strands would yield FRET >0.84 and <0.07, respectively. However, this is *at best* an approximation due to the unknown effect of BLM and/or BLM + hRPA on the conformations of the unwound strands. Therefore, we assessed the number of base pairs being unwound during these partial unwinding events by comparing repetitive unwinding parameters for FK34 versus another template, FK50a (Supplementary Figure S1D), in which the first 34 bp of the 50-bp duplex region were identical in sequence to the 34-mer duplex region of FK34 and the overall GC content was similar. The *Unwinding Times* for these two substrates with both core-BLM and WT-BLM were nearly identical (Supplementary Figure S5) showing that the maximal length of DNA being unwound per event is less than 34 bp and is not limited by the length of the duplex region in FK34.

Dependence of repetitive unwinding on BLM and ATP concentrations

Repetitive unwinding was observed over a wide range of ATP concentrations, from 1 μM to 2 mM. We focused on the ATP concentrations of 1–100 μM for which the relatively slow unwinding facilitated quantitative analysis. Data obtained with BLM concentrations exceeding 50 nM were not quantified because we observed significant reduction of fluorescent

spots over time indicating full unwinding, probably due to the action of multiple molecules of BLM. Our gel-based analysis also showed that only at high BLM concentrations above 50 nM, is a significant fraction of FK34 molecules unwound (Supplementary Figure S1). Supplementary Figure S6A displays the fraction of initially high FRET molecules that displayed repetitive unwinding as a function of core-BLM and ATP concentration. This percentage generally increased with increasing BLM concentration at ATP concentrations $\geqslant 5\,\mu M$ ATP. In the ranges of 5–10 nM BLM and 5–20 μM ATP, which are optimal for investigating repetitive unwinding, up to 40% of the molecules showed repetitive unwinding patterns. The remaining molecules stayed at high FRET until photobleaching or termination of data acquisition, most likely because they were not engaged by a catalytically active species of BLM.

As expected for an ATP-powered enzyme, *Unwinding Time* decreased with increasing ATP concentration (Figure 2A; Supplementary Figure S6B). *Unwinding Time*, however, did not depend on enzyme concentration for ATP concentrations $\geqslant 5\,\mu M$ (Supplementary Figure S6B), indicating that a well-defined species of BLM is responsible for repetitive unwinding. Dependence on ATP concentration and independence of enzyme concentration were also observed in the average values of each of the three subsegments of *Unwinding Time—Time per ΔFRET*, *Low FRET Time*, and *Reannealing Time* (Supplementary Figure S6C–E). Even though reannealing is rapid—4–5 times faster than *Time per ΔFRET* on

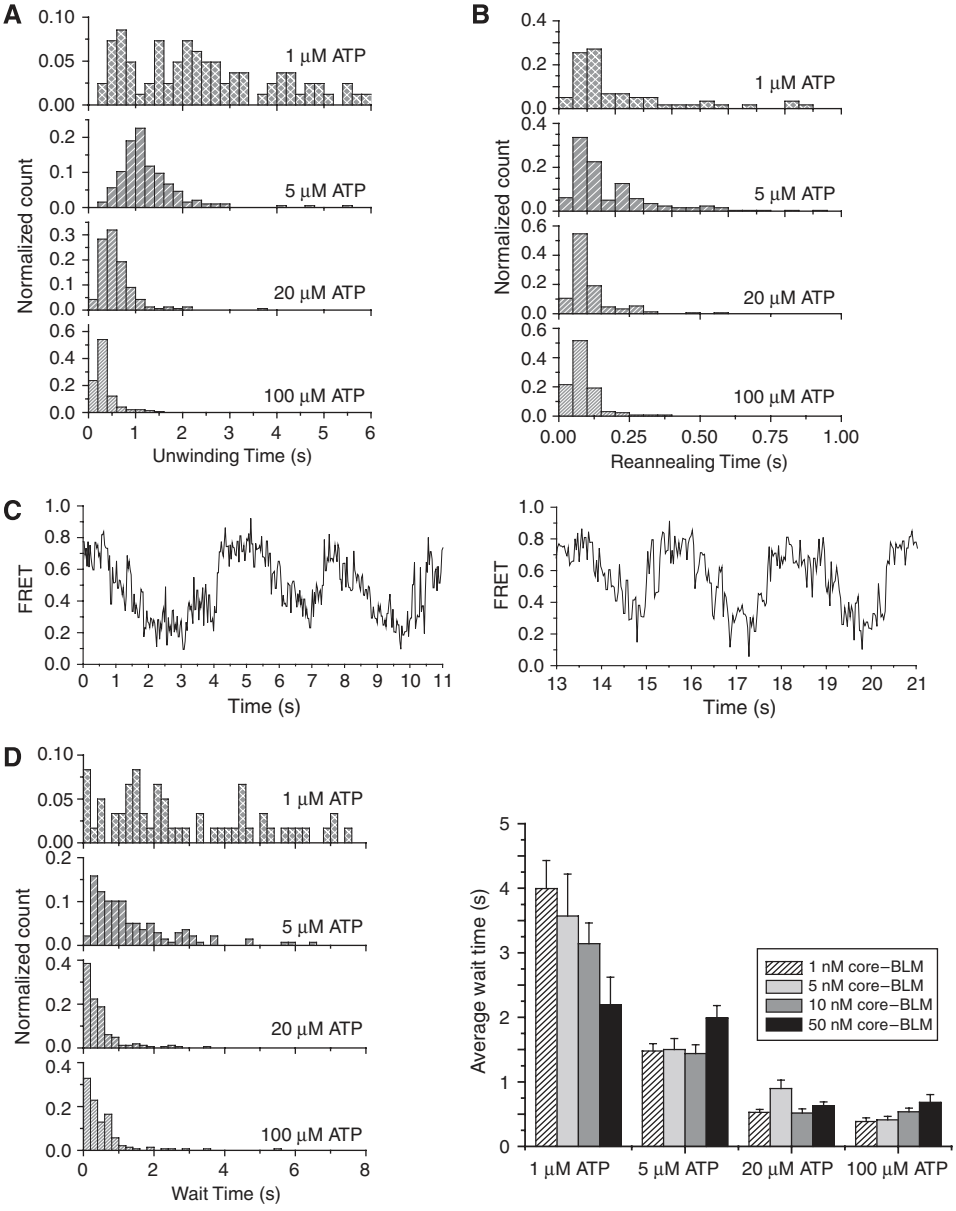

Figure 2 Dependence of repetitive unwinding of FK34 DNA on the concentrations of core-BLM and ATP. All histograms are normalized for the number of events, *n*. (**A**, **B**, **D** left panel) Measurements were taken at 10 nM core-BLM and 1–100 μM ATP. (A) Histogram of *Unwinding Times* (*n* range: 82–195). (B) Histogram of *Reannealing Times* (*n* range: 59–262). (**C**) Two representative smFRET traces measured at 10 nM core-BLM and 5 μM ATP demonstrating that reannealing is not instantaneous at low ATP concentration. (D) Dependence of *Wait Time* on BLM and ATP concentration. (Left panel) Histogram of *Wait Times* (*n* range: 60–166). (Right panel) Average *Wait Times* ± s.e. as a function of core-BLM (1–50 nM) and ATP (1–100 μM), (*n* range: 35–166). Please refer to Supplementary data 'Statistical methods' for calculation of error bars.

Table II Comparison of mean values for repetitive unwinding parameters

	Core-BLM				WT-BLM			
	−hRPA	+hRPA	Mean difference ± EMD	No. sigmas	−hRPA	+hRPA	Mean difference ± EMD	No. sigmas
Mean ΔFRET ± s.e.	0.317 ± 0.004	0.411 ± 0.004	0.094 ± 0.006	16.6	0.307 ± 0.0032	0.392 ± 0.005	0.085 ± 0.006	14.5
Mean Time per ΔFRET ± s.e.	0.441 ± 0.01	0.666 ± 0.018	0.225 ± 0.021	10.9	0.570 ± 0.014	0.654 ± 0.017	0.084 ± 0.022	3.9
Mean Low FRET Time ± s.e.	0.259 ± 0.013	0.439 ± 0.018	0.180 ± 0.022	8.2	0.218 ± 0.0156	0.406 ± 0.021	0.188 ± 0.026	7.2
Mean Unwinding Time ± s.e.	0.799 ± 0.009	0.945 ± 0.013	0.145 ± 0.016	9.1	0.873 ± 0.013	1.085 ± 0.023	0.211 ± 0.027	7.8
Mean Reannealing Time ± s.e.	0.111 ± 0.007	0.104 ± 0.007	0.007 ± 0.096	0.7	0.108 ± 0.006	0.096 ± 0.005	0.012 ± 0.008	1.5
Mean Wait Time ± s.e.	0.604 ± 0.028	2.29 ± 0.072	1.69 ± 0.077	21.8	0.925 ± 0.036	1.043 ± 0.069	0.117 ± 0.078	1.5

Mean (i.e. average) values correspond to the data shown in Figure 4 C and D and Supplementary Figure S9 measured at 10 nM BLM + 20 μM ATP, and 10 nM hRPA. s.e. = Std dev/$\sqrt{n}$ where n = number of measurements; mean difference (MD) = $|\text{Mean}_{+\text{RPA}} - \text{Mean}_{-\text{RPA}}|$; Error on mean difference (EMD) = $\sqrt{(\text{s.e.}_{-\text{RPA}})^2 + (\text{s.e.}_{+\text{RPA}})^2}$; Sigma = MD/EMD.

average (Table II)—it was not instantaneous within our time resolution and became slower as ATP concentration was lowered (Figure 2B and C), suggesting that the reannealing phase involves BLM translocation on ssDNA. Previous studies have shown that ssDNA translocation is much faster than unwinding in other helicases (Fischer *et al*, 2004; Jeong *et al*, 2004; Lionnet *et al*, 2007).

Wait Time is also dependent on ATP concentration

After DNA is rezipped, a finite time termed *Wait Time* elapses before unwinding reinitiates. The *Wait Time* decreased as ATP concentration increased (Figure 2D). Therefore, *Wait Time* may represent translocation on the ssDNA tail or an ATP-dependent reactivation step of BLM. The *Wait Times* at ATP $\geqslant$5 μM are independent of core-BLM concentrations. Therefore, successive unwinding events are not caused by enzyme dissociation followed by the binding of another enzyme. Rather, it appears that a single BLM species capable of unwinding remains bound to the same DNA molecule for multiple cycles of successive unwinding. Further supporting this interpretation, when the unwinding reaction was performed at high BLM concentration followed by a wash with a buffer containing only ATP to remove free BLM in solution, 15% of the molecules still exhibited repetitive unwinding behaviour (data not shown). At 1 μM ATP, the *Wait Times* did become longer at lower BLM concentration, indicating that BLM falls off the DNA more easily at very low ATP concentrations (Figure 2D).

The number of base pairs of DNA unwound before reannealing is narrowly distributed

Distributions of *ΔFRET*, the FRET change per unwinding event, showed a distinct peak at ~0.3 U (Figure 3A, left panel). When these data are integrated in the *ΔFRET* axis to calculate the accumulated unwinding events that reversed before reaching a particular *ΔFRET* value (Figure 3A, right panel), we obtained a pronounced lag phase clearly showing that reversal of unwinding becomes significant only after reaching a threshold *ΔFRET* (>0.2 U). This threshold, thus, represents a critical length of DNA unwound before reversal. This observation is inconsistent with the prevalent model that the rate with which unwinding terminates is independent of the total number of base pairs unwound because such a model predicts that the accumulated unwinding events that are reversed would increase from the very beginning of unwinding without a lag phase (Figure 3B, upper panel). Rather, our data suggest that BLM has a very low chance of terminating the unwinding reaction at early time points, but after it has unwound a critical number of base pairs, which is less than 34 bp, its chance of termination increases dramatically (Figure 3B, lower panel). As the FRET noise level, 0.08, is 2.5 times lower than the threshold *ΔFRET* (0.2), the low probability for unwinding termination between *ΔFRET* 0.1–0.2 cannot be attributed to the masking of events with small *ΔFRET* by noise. Also, the critical DNA length at which unwinding terminates is not sharply defined, for example with a single base pair precision, because *ΔFRET* ranged from 0.1–0.5 (Figure 3A, left panel), a range larger than that expected from noise alone. *ΔFRET* exhibited a positive correlation with *Time for ΔFRET* (Figure 3C), further suggesting that a significant source of broadening of *ΔFRET* distribution is indeed the variation in the extent of unwinding for each cycle.

Repetitive unwinding persists even in the presence of hRPA

Biochemical assays have shown that BLM-catalysed unwinding of duplexes that are hundreds of base pairs long requires the presence of hRPA (Brosh *et al*, 2000; Doherty *et al*, 2005). However, these studies were performed under multiple turnover conditions in which one cannot discern whether unwinding of long duplexes is catalysed upon a single binding event by an unwinding-competent BLM unit or whether it requires multiple BLM-binding events. Thus, we tested how hRPA affects the repetitive unwinding behaviour in our assay, which requires a single binding event of a BLM unit capable of unwinding.

Remarkably, repetitive unwinding persisted even in the presence of hRPA in solution for both WT-BLM (Figure 4A) and core-BLM (data not shown). The apparent robustness of repetitive unwinding cannot be attributed to the inability of hRPA to bind to the DNA because unwinding events in the presence of hRPA are generally longer and produce a greater FRET change (Figure 4A). This effect is maximal at 10 nM hRPA and was not dependent on whether hRPA is added prior to or simultaneously with BLM and ATP (data not shown). The effect of hRPA is not due to hRPA-induced duplex melting as no FRET change was observed in FK34 upon addition of 10 nM hRPA alone (Supplementary Figure S7). To quantify the effect of hRPA, we aligned each unwinding curve in time by setting the beginning of FRET decrease as time $t = 0$, and plotted the average FRET versus t, averaged over 300 unwinding events (Figure 4B). Comparison between the two

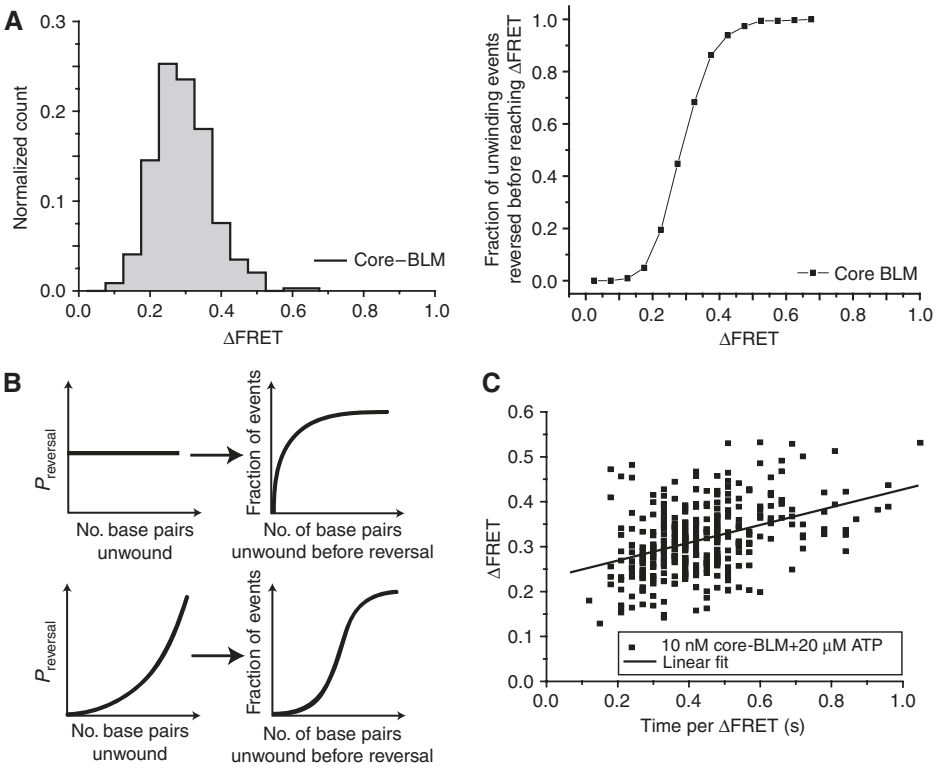

Figure 3 BLM 'measures' the number of base pairs unwound in each unwinding cycle. (**A**, left panel) Normalized histogram of *ΔFRET* values measured for ($n = 344$) unwinding events at 10 nM core-BLM + 20 μM ATP. (A, right panel) Fraction of unwinding events reversed before reaching *ΔFRET* versus *ΔFRET* calculated from (A, left panel). (**B**) Illustration of how BLM 'measures' number of base pairs unwound. (Top panel) For a helicase in which the probability of reversal of unwinding (P_r) is independent of the number of base pairs unwound, the accumulated unwinding events that are reversed would be predicted to increase from the very beginning of unwinding. (Bottom panel) For a helicase in which the P_r increases significantly after it has unwound a critical number of base pairs, the accumulated unwinding events that are reversed would be predicted to significantly increase only upon reaching a threshold *ΔFRET* (i.e. base pairs unwound), consistent with our data in (A, right panel). (**C**) Plot of *ΔFRET* as a function of time per *ΔFRET* (for data shown in (A); Linear fit yields y-int = 0.229 ± 0.01; slope = 0.198 ± 0.022; $r = 0.437$; $P < 0.001$).

FRET curves with and without hRPA shows clearly that hRPA allows unwinding to proceed to a lower final average FRET value. hRPA also shifts the *ΔFRET* distribution towards higher values (Supplementary Figures S8A and S9A). This effect of hRPA may come from both the enhanced processivity and the stretching of ssDNA being generated during unwinding. Using partial duplex 3′ ss-tailed substrates, we found that hRPA does stretch ssDNA and that it binds less stably to a 13-nt tail and very stably to tails >21 nt (Supplementary Figure S10).

hRPA facilitates reinitiation of unwinding by WT-BLM

Does hRPA change only the FRET values without any effect on the kinetics of repetitive unwinding? The answer appears to be 'no' because three of the *Unwinding Time* parameters, *Unwinding Time*, *Time per ΔFRET*, and *Low FRET Time* increased when hRPA was included (Supplementary Figure S8B–D). Similar trends are also observed with core-BLM (Figure 4C; Supplementary Figure S9B and C, Table II). However, *Reannealing Time* does not depend on hRPA (Supplementary Figures S8E and S9D; Table II), indicating that hRPA is easily displaced before or during reannealing.

Interestingly, hRPA increased the *Wait Time* for core-BLM but not for WT-BLM (Figure 4D–F; Table II). To ensure that this differential effect of hRPA is not due to a situation where either hRPA or core-BLM are at concentrations lower than their respective K_d values for their interaction (Doherty *et al*, 2005), we confirmed that the *Wait Time* effect still persists at higher saturating levels of core-BLM (25–50 nM; Figure 4D, CB5–50) and hRPA (50 nM; Figure 4D, light grey columns). This effect is most likely due to the fact that WT-BLM has a high-affinity hRPA-binding domain in its N terminus that is missing in core-BLM (Doherty *et al*, 2005). Thus, after reannealing core-BLM is less able than WT-BLM to either bind hRPA and reinitiate translocation as a complex or to compete with hRPA for access to the 3′ tail. We conclude that direct interaction between WT-BLM and hRPA is needed for efficient reinitiation of unwinding of hRPA-coated DNA.

Discussion

smFRET reveals repetitive DNA unwinding by BLM

The study presented is the first single-molecule study of a RecQ family helicase. Unlike gel-based assays, our smFRET assay was able to detect partially unwound intermediates in real time, leading to the discovery of 'repetitive unwinding' where BLM catalyses multiple unwinding events in succession on a single DNA molecule. The BLM and ATP concentration dependence of this behaviour suggests that repetitive partial unwinding is the norm that should be expected from a minimal unit capable of unwinding, and that full unwinding events are most likely to be caused by the action of more than

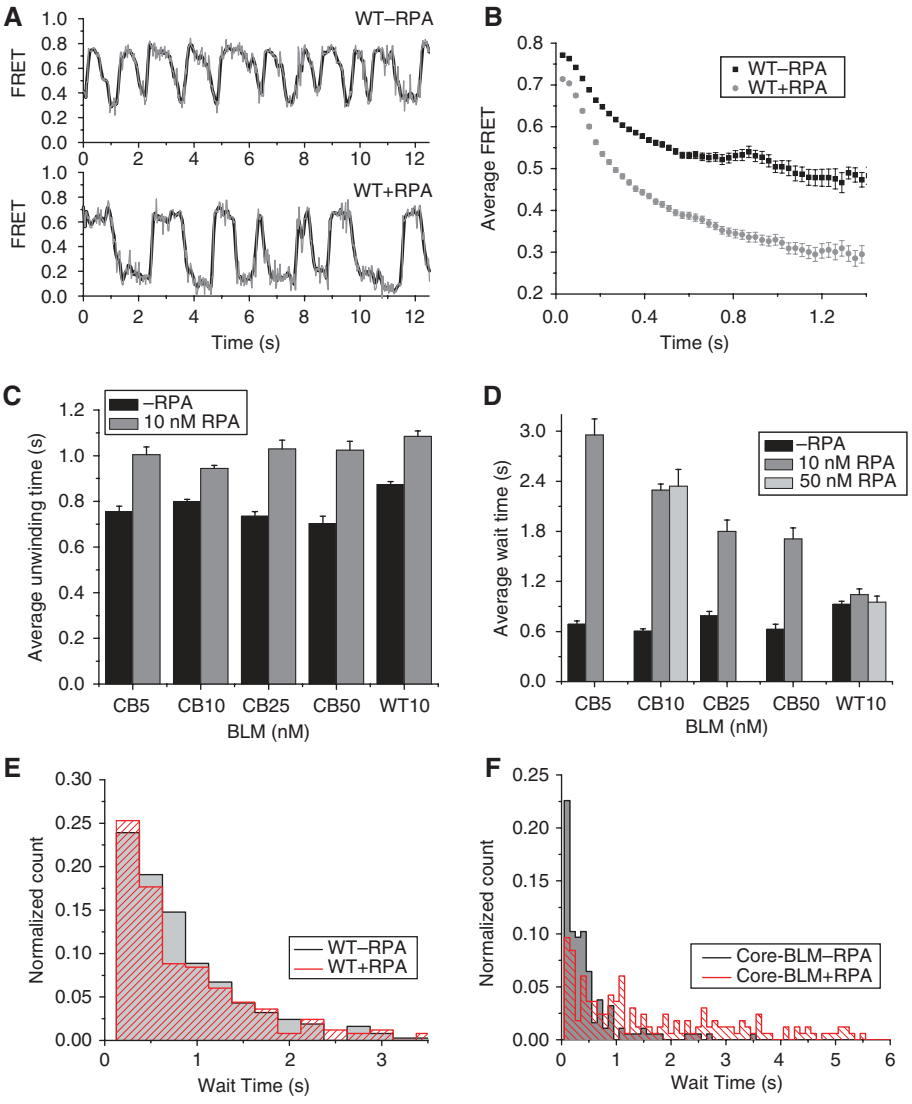

Figure 4 Effect of hRPA on repetitive unwinding of FK34 DNA by core-BLM and WT-BLM. (**A**) Representative smFRET time traces of unwinding by 10 nM WT-BLM (WT10) at 20 μM ATP in the absence (upper panel) and presence (lower panel) of 10 nM hRPA. Raw time traces are shown in grey, whereas the three-point averaged traces are shown in black. (**B**) FRET decay time course averaged from (n) unwinding events (measured in (A)) in the absence (black, $n = 330$) and presence (grey, $n = 335$) of 10 nM hRPA. Error bars represented the s.e. calculated at each time point (t). Time courses begin at $t = 0$ when n is at the highest value and end at t when $n = 10$. For (**C**, **D**), experiments were performed at 5–50 nM core-BLM (CB5–50) and 10 nM WT-BLM (WT10) + 20 μM ATP (black columns) ± 10 nM hRPA (grey columns) or 50 nM hRPA (light grey columns); N = number of experiments; n = number of measurements. Please refer to Supplementary data 'Statistical methods' for calculation of error bars. (C) Average *Unwinding Time* ± s.e.: N range:1–4; n range: 90–625. (D) Average *Wait Time* ± s.e.: N range: 1–2; n range: 63–495. (**E**) Normalized histograms of *Wait Time* for WT-BLM (10 nM) at 20 μM ATP: (−hRPA, black) $n = 372$; (+10 nM hRPA, red) $n = 277$. (**F**) Normalized histograms of *Wait Time* for core-BLM (10 nM) at 20 μM ATP: (−hRPA, black) $n = 166$; (+10 nM hRPA, red) $n = 186$.

one BLM. BLM concentration did not affect the time parameters of repetitive unwinding, suggesting that a single BLM species carries out successive unwinding events per single DNA-binding event. Repetitive unwinding was observed with WT-BLM and core-BLM ($BLM^{642–1290}$), a mutant that lacks the oligomerization domain, leading us to conclude that the minimal unit sufficient for repetitive unwinding is a monomeric species that comprises the RecQ catalytic core of BLM. Repetitive behaviour was first discovered in ssDNA translocation by *E. coli* Rep helicase (Myong *et al*, 2005) and then in DNA unwinding by HCV NS3 helicase (Myong *et al*, 2007), but until now no detailed mechanism of repetitive unwinding has been reported.

Strand-switching model for repetitive unwinding by BLM

Increasing ATP concentration shortened the time per unwinding event (*Unwinding Time*) as well as the time elapsed between unwinding events (*Wait Time*). Although the ATP dependence of the first two phases of unwinding (*Time per ΔFRET* and *Low FRET Time*) most likely represents ATP-powered separation of duplex DNA, the ATP dependence of phase III, *Reannealing Time*, suggests that ATP-powered translocation along ssDNA occurs during this phase also. One possibility is that the helicase reverses polarity during the course of unwinding and translocates 5′–3′ on the tracking strand with the concomitant reannealing of the unwound

strands. This option seems highly unlikely given the numerous substrate specificity studies indicating that BLM requires a 3′ tail for unwinding as well as the fact that, to date, no 5′–3′ directionality has been detected for BLM (Karow *et al*, 1997; Mohaghegh *et al*, 2001). We favour a different scenario in which BLM switches strands and translocates 3′–5′ along the displaced strand accompanied by reannealing of the strands in its wake.

In our model (Figure 5A), we propose that the catalytic core of BLM is associated with the DNA junction in a similar manner to how the *E. coli* RecQ crystal structure has been modelled to interact with a ssDNA–dsDNA junction (Bernstein *et al*, 2003), with the RecQ-Ct domain interacting with the duplex region, whereas the 3′ tail is bound by the helicase 1A and 2A domains. Although this mode of BLM–DNA interaction is speculative and used mainly for illustra-

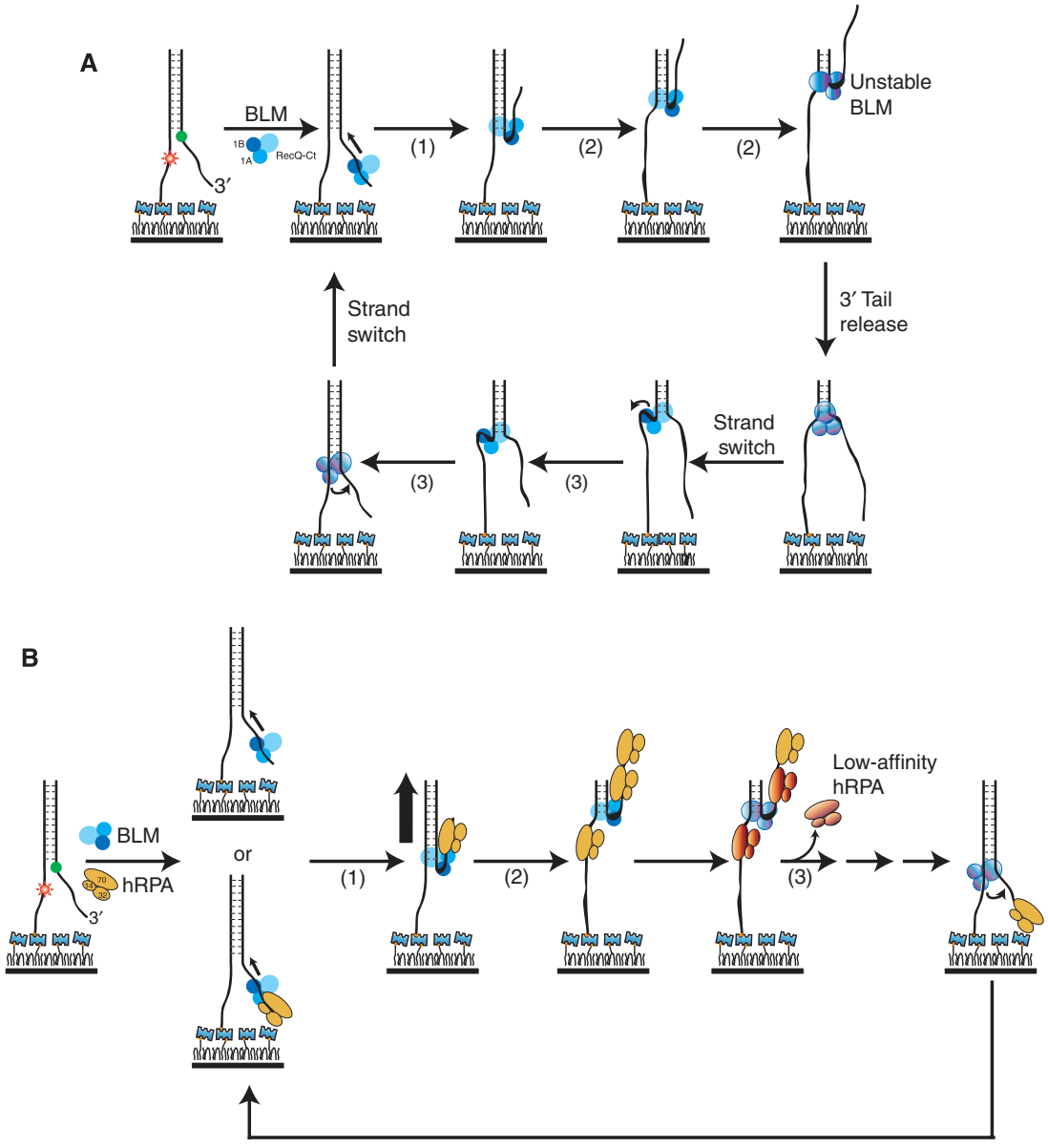

Figure 5 Strand-switching model for repetitive unwinding by BLM. (**A**) (−hRPA): BLM depicted comprises only the catalytic core bound to DNA in a manner similar to model proposed for *E. coli* RecQ: Domains 1A (blue), 1B (dark blue), and RecQ-Ct (light blue). BLM binds and translocates on the 3′ ss tail to the junction (step (1)) and initiates unwinding with continued translocation on the tracking strand (step (2)). After unwinding, a critical length of DNA, BLM may enter a state (gradient blue) where it remains attached to the duplex DNA through its RecQ-Ct domain, but releases the 3′ ss tail from its helicase domains and switches to bind the newly generated 5′ ss tail. BLM proceeds to translocate along this strand in the 3′–5′ direction with the single strands reannealing in its wake (step (3)). When the duplex is fully reformed, BLM rebinds the 3′ tail and translocates towards the junction whereupon it can reinitiate the unwinding cycle (step (1)). (**B**) (+hRPA): hRPA heterotrimer (gold); RPA70 subunit (70), RPA32 subunit (32), and RPA14 subunit (14) are depicted in its compact lower affinity mode. In the presence of hRPA, a BLM–hRPA complex forms either in solution or on the DNA (step (1)). In this complex, BLM can unwind further through the duplex (represented by the heavy black arrow, (step (2)). When BLM stops after unwinding a critical length and switches strands, the low-affinity form of hRPA (gradient orange) is likely displaced *at least* from newly unwound regions of DNA (step (3)). After completion of reannealing, BLM transfers back to the 3′ tail, aided (in the case of WT-BLM) by its physical interaction with the hRPA bound to the 3′ tail, and begins a new cycle of unwinding.

tive purposes, the key point for our model is that *some* portion of BLM remains bound to the DNA throughout the entire repetitive unwinding event. BLM binds and translocates on the 3′ ss tail to the junction (step (1)) and initiates unwinding with continued translocation on the tracking strand (step (2)). After unwinding a critical length of DNA, BLM may enter a state where it remains attached to the duplex DNA, but releases the 3′ ss tail from its helicase domains and switches to bind the newly generated 5′ ss tail. BLM will then proceed to translocate along this strand in the 3′–5′ direction, with the single strands reannealing in its wake (step (3)). When the duplex is fully re-formed, BLM may enter a state in which its helicase domains release the 5′ tail and rebind the 3′ tail that is now in closer proximity. BLM will then reinitiate translocation along the 3′ tail towards the junction corresponding to the *Wait Time* in our system (step (1)), consistent with the ATP dependence of this parameter. The wide distribution in *Wait Times* (Figure 2D, left panel) suggests that the position along the 3′ tail where BLM rebinds is variable. Further evidence that 3′ tail translocation occurs during the *Wait Time* period is the observation that *Wait Time* was 30% longer with a 60-nt 3′ tail versus a 30 nt 3′ tail (Supplementary Figure S11). Once the 3′ ss tail translocation is completed, BLM can now reinitiate the unwinding cycle.

Low processivity of BLM

Unlike in previous ensemble measurements that showed unwinding of hundreds of base pairs by BLM in the presence of hRPA (Brosh *et al*, 2000), the minimal catalytically active unit of BLM in our single-molecule experiments did not unwind more than 34 bp even in the presence of hRPA. This difference is most likely due to the action of multiple BLM proteins working in conjunction in the ensemble studies. A possible mechanism leading to BLM reversal after unwinding a critical length of duplex may involve the reannealing of the newly unwound strands behind the helicase, which may destabilize BLM–substrate interactions causing BLM to partially disengage from the DNA. Alternatively, BLM may remain attached to the tracking or non-tracking strand during unwinding such that a ssDNA loop forms as it unwinds, creating a topological constraint, which is relieved after unwinding a critical length, reminiscent of a model proposed for the hepatitis C virus NS3 helicase (Serebrov and Pyle, 2004; Myong *et al*, 2007). The strand reannealing proposed to occur in the wake of BLM translocation on the opposing strand is probably unrelated to the reported intrinsic BLM ssDNA annealing activity (Cheok *et al*, 2005; Machwe *et al*, 2005) because this annealing activity is inhibited by hRPA, which we do not observe (Supplementary Figures S8E and S9D), and is inhibited by ATP that is present in under our conditions, and because it requires C-terminal residues 1290–1350, which are missing in core-BLM.

Comparison to other helicases

In magnetic tweezers-based single-molecule assays (Dessinges *et al*, 2004), it was observed that UvrD-catalysed DNA unwinding becomes highly processive and rapid when high force is applied to the DNA, in sharp contrast to the much slower and less processive unwinding reported in ensemble studies performed without applied force (Maluf *et al*, 2003). It was also found that when the unwinding reaction terminates at random locations on the DNA, the UvrD helicase can switch strands to translocate on the other strand, causing DNA rezipping that occurred at the same speed as unwinding (Dessinges *et al*, 2004). Strand switching by BLM observed in our study is distinct from that of UvrD in two important aspects. First, we found that unwinding is much slower than reannealing, most likely due to the absence of applied force, which we argue is more relevant physiologically than the presence of 20 pN force in the UvrD single-molecule study. More importantly, BLM unwinding reverses at a relatively well-defined position from the beginning of unwinding, which is in strong contrast to the stochastic termination behaviour of UvrD. Similarly, gradual reannealing of DNA was observed from a single-molecule mechanical analysis of T7 helicase after unwinding a random number of base pairs (Johnson *et al*, 2007). It appears that, unlike UvrD or T7 helicase, BLM is able to 'measure' how many base pairs it has unwound, and once it has unwound a critical length, it rapidly reverses the unwinding reaction through strand switching.

hRPA produces a limited enhancement in processivity

We examined the effect of hRPA on BLM's ability to catalyse repetitive unwinding. hRPA is a natural partner of BLM and physically interacts with BLM through specific domains on both proteins (Brosh *et al*, 2000; Doherty *et al*, 2005). Direct physical interaction between the two proteins may enable WT-BLM to unwind long duplexes (Brosh *et al*, 2000) and to unwind vinylphosphonate-containing substrates (Garcia *et al*, 2004).

We found that hRPA does not eliminate the ability of BLM to unwind repetitively on short duplexes. Nevertheless, hRPA does produce a distinct effect in unwinding of short duplexes as demonstrated by the small but definite increases in duration of the unwinding reaction, and by the more pronounced FRET change during unwinding. The increase in *Unwinding Time* mostly likely reflects an increase in processivity, although we cannot completely rule out the possibility that hRPA may decrease the unwinding speed without any change in processivity.

It was shown previously that BLM-catalysed DNA unwinding is also stimulated by *Saccharomyces cerevisiae* RPA (scRPA), a homlogue of hRPA, but not by *E. coli* SSB, which is structurally distinct from hRPA (Brosh *et al*, 2000). We also found that scRPA can produce the same effect as hRPA in our single-molecule experiments, whereas *E. coli* SSB inhibits unwinding by BLM (data not shown). Therefore, the effect of hRPA on unwinding processivity is most likely to be through a direct hRPA–BLM interaction instead of a more general blockage of reannealing. Because the unwinding characteristics are similar for core-BLM and WT-BLM, a lower affinity C-terminal hRPA-binding site, which is still present in core-BLM (Doherty *et al*, 2005), would be responsible for the modest enhancement of unwinding processivity in the presence of hRPA.

hRPA allows reannealing and facilitates unwinding reinitiation by WT-BLM

Interestingly, hRPA does not appear to present any barrier against reannealing after strand switching because we found that *Reannealing Time* is unaffected by the presence of hRPA (Supplementary Figures S8E and S9D). Combined with our results showing that hRPA dissociates much more readily from a 13-nt 3′ tail compared with the tails longer than 21 nt

(Supplementary Figure S10), it is most likely that, at least in the fork region, hRPA may be bound in a lower affinity compact mode (Fanning *et al*, 2006) so that hRPA is easily displaced by BLM upon reannealing.

After completion of reannealing, BLM needs to transfer back to the 3′ tail before reinitiation of unwinding. Our observation that hRPA increases *Wait Time* only for core-BLM (Figure 4D and F) suggests that reinitiation of unwinding by core-BLM is inhibited by the occlusion of the 3′ tail by hRPA; in contrast, the hRPA interaction domain in the N terminus of the WT-BLM facilitates the transfer of the helicase from the 5′ tail to the 3′ tail for efficient reinitiation of unwinding.

Our model for repetitive unwinding in the presence of hRPA is presented in Figure 5B. A BLM–hRPA complex forms either in solution or on the DNA (step (1)). In this complex, BLM can unwind further through the duplex (represented by the heavy black arrow, (step (2)). When BLM stops after unwinding a critical length and switches strands, hRPA is most likely displaced *at least* from newly unwound regions of DNA (step (3)). After completion of reannealing, BLM transfers back to the 3′ tail, aided by its physical interaction with the hRPA bound to the 3′ tail, and begins a new cycle of unwinding.

Biological implications of BLM repetitive unwinding and strand switching

The finding that BLM, a human RecQ homologue, is able to switch strands while unwinding a forked substrate may provide a rationalization of the results of a previous study on processing of stalled replication forks by *E. coli* RecQ (Hishida *et al*, 2004). Their study revealed that RecQ preferentially binds substrates with a leading strand gap and converts these into structures with a lagging strand gap. This was postulated to occur through strand switching and 3′–5′ translocation along the lagging strand template. Our results provide strong evidence for strand switching by a human RecQ helicase and, moreover, demonstrate that a single BLM molecule translocates in succession on each strand. BLM strand switching could also have a function in the recovery of stalled replication forks by either BLM-promoted fork regression (Machwe *et al*, 2006; Ralf *et al*, 2006) through chicken-foot intermediate formation and/or BLM-promoted replication fork restart through its reverse branch migration activity on chicken-foot intermediates (Karow *et al*, 2000).

BLM's ability to measure the length of unwound DNA before reversal by strand switching may also have a function in heteroduplex rejection during early stages of HR. For example, in conjunction with mismatch repair (MMR) machinery, BLM may begin to unwind D-loops formed at an early point in strand invasion, while checking for homology. If the sequences turn out to be slightly divergent, BLM will continue to unwind the intermediate, preventing HR. However, if after unwinding a certain number of base pairs, BLM and MMR machinery confirm the legitimacy of the recombination intermediate, then BLM could terminate unwinding by switching to the invading strand and translocating 3′–5′ along that strand so that HR could continue. Thus, when strand invasion resumes in another location, BLM will be situated to begin the 'checking' process again. Evidence supporting the role of RecQ helicases working with MMR proteins to prevent recombination between divergent sequences has been shown for *S. cerevisiae* Sgs1 (Sugawara *et al*, 2004; Goldfarb and Alani, 2005) and for human WRN (Saydam *et al*, 2007). In addition, direct interactions between BLM and MMR proteins have been observed *in vitro* and *in vivo* (Bachrati and Hickson, 2003).

BLM may also use its strand-switching ability to displace proteins during replication fork repair and HR. One possible displacement candidate suggested by our results is hRPA. Such protein-mediated hRPA displacement has been proposed to occur in the SV40 replication pathway (Fanning *et al*, 2006) and during Rad51 filament assembly (Kantake *et al*, 2003; Stauffer and Chazin, 2004). Another likely displacement candidate is hRAD51 as BLM has been demonstrated to directly interact with RAD51 (Braybrooke *et al*, 2003) and disrupt RAD51 filament formation (Bugreev *et al*, 2007). Strand switching by the SRS2 helicase has been proposed to have a function in RAD51 displacement during the synthesis-dependent strand annealing pathway (Dupaigne *et al*, 2008). In the light of our findings, it is plausible that BLM may perform a similar function *in vivo*.

Materials and methods

Preparation of DNA substrates

Oligonucleotides were purchased from Integrated DNA Technologies (Coralville, IA). The sequences and modifications for the substrates discussed are presented in Table I. Oligonucleotides with Cy5 at internal positions were backbone-labelled using phosphoramidite chemistry, whereas oligonucleotides with internal Cy3 contained an amino modifier at the specified position that was subsequently labelled using Cy3 monofunctional NHS esters according to Joo and Ha (2008). In substrates where the duplex faced away from the surface, the biotinylated strand was the non-tracking strand except for the NonFK50-3′-tether substrate.

Forked and non-forked partial duplex substrates were prepared by mixing the appropriate biotinylated and non-biotinylated oligonucleotides in a 1:1.5 molar ratio at 10 μM in T50 buffer (10 mM Tris (pH 8.0) and 200 mM NaCl). Annealing reactions were incubated at 95°C for 3 min followed by slow cooling to room temperature for 3 h.

Proteins

Truncation mutant $BLM^{642-1290}$ (core-BLM) encompassing the region homologous to the RecQ catalytic core, was purified as previously described (Janscak *et al*, 2003). WT-BLM was purified as described (Kanagaraj *et al*, 2006). Recombinant human (hRPA) and *S. cerevisiae* (scRPA) were provided by Marc Wold (Henricksen *et al*, 1994). *E. coli* SSB (Lohman and Ferrari, 1994) was provided by Tim Lohman.

Single-molecule FRET assay

smFRET measurements were performed using a wide-field total internal reflection fluorescence microscope (Joo and Ha, 2008). Total internal reflection excitation was carried out through an objective (Olympus UplanSApo; × 100 numerical aperture; 1.4 oil immersion). Images were acquired at 30-ms time resolution using an electron multiplying charge-coupled device camera (iXon DV887-BI; Andor Technology) and a home-made C++ program. FRET values were calculated as the ratio between acceptor intensity and the sum of the donor and acceptor intensities after correcting for donor leakage between the two detection channels and subtracting the background (Ha *et al*, 2002; Rasnik *et al*, 2004).

Quartz slides and glass cover slips were surface-passivated with PEG (Nektar Therapeutics) containing 1% (w/w) biotin-PEG (Laysan Bio. Inc.) as described (Ha *et al*, 2002; Rasnik *et al*, 2004). After verifying the surface integrity, neutravidin (Thermo Scientific) was added as described (Joo and Ha, 2008) followed by the addition of 100–200 pM biotinylated Cy3- and Cy5-labelled DNA substrate. After washing off any unbound DNA, immobilized DNA was imaged in BLM unwinding buffer (Karow *et al*, 1997; Brosh *et al*, 2000) containing 50 mM Tris–HCl (pH 7.5), 50 mM NaCl, 5 mM $MgCl_2$, 50 μg/ml BSA, 1 mM DTT, an oxygen scavenger

system containing 0.8% dextrose, 0.1 mg/ml glucose oxidase (Sigma-Aldrich), 0.02 mg/ml catalase (Roche) (Joo and Ha, 2008), and 1.5 mM Trolox (Sigma-Aldrich), a triplet-quenching agent (Rasnik *et al*, 2006). Unwinding reactions, initiated by the simultaneous addition of BLM and ATP, were carried out and imaged at room temperature in BLM unwinding buffer containing ATP (1 μM–2 mM), BLM (1–100 nM, monomer) ± hRPA (10 or 50 nM, heterotrimer).

Supplementary data

Supplementary data are available at *The EMBO Journal* Online (http://www.embojournal.org).

Acknowledgements

We thank Eli Rothenberg, Jeehae Park, Sinan Arslan, and Maria Spies for helpful scientific discussions as well as assistance with data analysis (ER and SA), and Sua Myong for her contributions during the initial phase of this study. We thank Marc Wold for providing hRPA and scRPA, and Tim Lohman for providing *E. coli* SSB. This study was supported, in part, by National Institutes of Health Grant GM065367 and National Science Foundation Grant 0822613 (to TH), by University of Illinois at Urbana-Champaign School of Molecular and Cellular Biology (to JGY) and by The Swiss National Science Foundation (to RK and PJ).

References

Bachrati CZ, Hickson ID (2003) RecQ helicases: suppressors of tumorigenesis and premature aging. *Biochem J* **374:** 577–606

Bachrati CZ, Hickson ID (2006) Analysis of the DNA unwinding activity of RecQ family helicases. *Methods Enzymol* **409:** 86–100

Bachrati CZ, Hickson ID (2008) RecQ helicases: guardian angels of the DNA replication fork. *Chromosoma* **117:** 219–233

Beresten SF, Stan R, van Brabant AJ, Ye T, Naureckiene S, Ellis NA (1999) Purification of overexpressed hexahistidine-tagged BLM N431 as oligomeric complexes. *Protein Expr Purif* **17:** 239–248

Bernstein DA, Zittel MC, Keck JL (2003) High-resolution structure of the *E. coli* RecQ helicase catalytic core. *EMBO J* **22:** 4910–4921

Braybrooke JP, Li JL, Wu L, Caple F, Benson FE, Hickson ID (2003) Functional interaction between the Bloom's syndrome helicase and the RAD51 paralog, RAD51L3 (RAD51D). *J Biol Chem* **278:** 48357–48366

Brosh Jr RM, Li JL, Kenny MK, Karow JK, Cooper MP, Kureekattil RP, Hickson ID, Bohr VA (2000) Replication protein A physically interacts with the Bloom's syndrome protein and stimulates its helicase activity. *J Biol Chem* **275:** 23500–23508

Bugreev DV, Yu X, Egelman EH, Mazin AV (2007) Novel pro- and anti-recombination activities of the Bloom's syndrome helicase. *Genes Dev* **21:** 3085–3094

Cheok CF, Wu L, Garcia PL, Janscak P, Hickson ID (2005) The Bloom's syndrome helicase promotes the annealing of complementary single-stranded DNA. *Nucleic Acids Res* **33:** 3932–3941

Dessinges MN, Lionnet T, Xi XG, Bensimon D, Croquette V (2004) Single-molecule assay reveals strand switching and enhanced processivity of UvrD. *Proc Natl Acad Sci USA* **101:** 6439–6444

Doherty KM, Sommers JA, Gray MD, Lee JW, von Kobbe C, Thoma NH, Kureekattil RP, Kenny MK, Brosh Jr RM (2005) Physical and functional mapping of the replication protein a interaction domain of the Werner and Bloom syndrome helicases. *J Biol Chem* **280:** 29494–29505

Dupaigne P, Le Breton C, Fabre F, Gangloff S, Le Cam E, Veaute X (2008) The Srs2 helicase activity is stimulated by Rad51 filaments on dsDNA: implications for crossover incidence during mitotic recombination. *Mol Cell* **29:** 243–254

Fanning E, Klimovich V, Nager AR (2006) A dynamic model for replication protein A (RPA) function in DNA processing pathways. *Nucleic Acids Res* **34:** 4126–4137

Fischer CJ, Maluf NK, Lohman TM (2004) Mechanism of ATP-dependent translocation of *E. coli* UvrD monomers along single-stranded DNA. *J Mol Biol* **344:** 1287–1309

Garcia PL, Bradley G, Hayes CJ, Krintel S, Soultanas P, Janscak P (2004) RPA alleviates the inhibitory effect of vinylphosphonate internucleotide linkages on DNA unwinding by BLM and WRN helicases. *Nucleic Acids Res* **32:** 3771–3778

Goldfarb T, Alani E (2005) Distinct roles for the *Saccharomyces cerevisiae* mismatch repair proteins in heteroduplex rejection, mismatch repair and nonhomologous tail removal. *Genetics* **169:** 563–574

Ha T, Rasnik I, Cheng W, Babcock HP, Gauss GH, Lohman TM, Chu S (2002) Initiation and re-initiation of DNA unwinding by the *Escherichia coli* Rep helicase. *Nature* **419:** 638–641

Hanada K, Hickson ID (2007) Molecular genetics of RecQ helicase disorders. *Cell Mol Life Sci* **64:** 2306–2322

Handa N, Bianco PR, Baskin RJ, Kowalczykowski SC (2005) Direct visualization of RecBCD movement reveals cotranslocation of the RecD motor after chi recognition. *Mol Cell* **17:** 745–750

Henricksen LA, Umbricht CB, Wold MS (1994) Recombinant replication protein A: expression, complex formation, and functional characterization. *J Biol Chem* **269:** 11121–11132

Hishida T, Han YW, Shibata T, Kubota Y, Ishino Y, Iwasaki H, Shinagawa H (2004) Role of the *Escherichia coli* RecQ DNA helicase in SOS signaling and genome stabilization at stalled replication forks. *Genes Dev* **18:** 1886–1897

Janscak P, Garcia PL, Hamburger F, Makuta Y, Shiraishi K, Imai Y, Ikeda H, Bickle TA (2003) Characterization and mutational analysis of the RecQ core of the bloom syndrome protein. *J Mol Biol* **330:** 29–42

Jeong YJ, Levin MK, Patel SS (2004) The DNA-unwinding mechanism of the ring helicase of bacteriophage T7. *Proc Natl Acad Sci USA* **101:** 7264–7269

Johnson DS, Bai L, Smith BY, Patel SS, Wang MD (2007) Single-molecule studies reveal dynamics of DNA unwinding by the ring-shaped T7 helicase. *Cell* **129:** 1299–1309

Joo C, Ha T (2008) Single-molecule FRET with total internal reflection microscopy. In *Single Molecule Techniques: a Laboratory Manual*, Selvin PR, Ha T (eds) pp 3–35 Cold Spring Harbor: Cold Spring Harbor Laboratory Press

Kanagaraj R, Saydam N, Garcia PL, Zheng L, Janscak P (2006) Human RECQ5beta helicase promotes strand exchange on synthetic DNA structures resembling a stalled replication fork. *Nucleic Acids Res* **34:** 5217–5231

Kantake N, Sugiyama T, Kolodner RD, Kowalczykowski SC (2003) The recombination-deficient mutant RPA (rfa1-t11) is displaced slowly from single-stranded DNA by Rad51 protein. *J Biol Chem* **278:** 23410–23417

Karow JK, Chakraverty RK, Hickson ID (1997) The Bloom's syndrome gene product is a 3′–5′ DNA helicase. *J Biol Chem* **272:** 30611–30614

Karow JK, Constantinou A, Li JL, West SC, Hickson ID (2000) The Bloom's syndrome gene product promotes branch migration of holliday junctions. *Proc Natl Acad Sci USA* **97:** 6504–6508

Karow JK, Newman RH, Freemont PS, Hickson ID (1999) Oligomeric ring structure of the Bloom's syndrome helicase. *Curr Biol* **9:** 597–600

Lee JB, Hite RK, Hamdan SM, Xie XS, Richardson CC, van Oijen AM (2006) DNA primase acts as a molecular brake in DNA replication. *Nature* **439:** 621–624

Lionnet T, Spiering MM, Benkovic SJ, Bensimon D, Croquette V (2007) Real-time observation of bacteriophage T4 gp41 helicase reveals an unwinding mechanism. *Proc Natl Acad Sci USA* **104:** 19790–19795

Lohman TM, Ferrari ME (1994) *Escherichia coli* single-stranded DNA-binding protein: multiple DNA-binding modes and cooperativities. *Annu Rev Biochem* **63:** 527–570

Machwe A, Xiao L, Groden J, Matson SW, Orren DK (2005) RecQ family members combine strand pairing and unwinding activities to catalyze strand exchange. *J Biol Chem* **280:** 23397–23407

Machwe A, Xiao L, Groden J, Orren DK (2006) The Werner and Bloom syndrome proteins catalyze regression of a model replication fork. *Biochemistry* **45:** 13939–13946

Maluf NK, Fischer CJ, Lohman TM (2003) A dimer of *Escherichia coli* UvrD is the active form of the helicase *in vitro*. *J Mol Biol* **325:** 913–935

Mohaghegh P, Karow JK, Brosh Jr RM, Bohr VA, Hickson ID (2001) The Bloom's and Werner's syndrome proteins are DNA structure-specific helicases. *Nucleic Acids Res* **29:** 2843–2849

Murphy MC, Rasnik I, Cheng W, Lohman TM, Ha T (2004) Probing single-stranded DNA conformational flexibility using fluorescence spectroscopy. *Biophys J* **86:** 2530–2537

Myong S, Bruno MM, Pyle AM, Ha T (2007) Spring-loaded mechanism of DNA unwinding by hepatitis C virus NS3 helicase. *Science* **317:** 513–516

Myong S, Rasnik I, Joo C, Lohman TM, Ha T (2005) Repetitive shuttling of a motor protein on DNA. *Nature* **437:** 1321–1325

Opresko PL, Cheng WH, Bohr VA (2004) Junction of RecQ helicase biochemistry and human disease. *J Biol Chem* **279:** 18099–18102

Perkins TT, Li HW, Dalal RV, Gelles J, Block SM (2004) Forward and reverse motion of single RecBCD molecules on DNA. *Biophys J* **86:** 1640–1648

Ralf C, Hickson ID, Wu L (2006) The Bloom's syndrome helicase can promote the regression of a model replication fork. *J Biol Chem* **281:** 22839–22846

Rasnik I, McKinney SA, Ha T (2006) Nonblinking and long-lasting single-molecule fluorescence imaging. *Nat Methods* **3:** 891–893

Rasnik I, Myong S, Cheng W, Lohman TM, Ha T (2004) DNA-binding orientation and domain conformation of the *E. coli* rep helicase monomer bound to a partial duplex junction: single-molecule studies of fluorescently labeled enzymes. *J Mol Biol* **336:** 395–408

Saydam N, Kanagaraj R, Dietschy T, Garcia PL, Pena-Diaz J, Shevelev I, Stagljar I, Janscak P (2007) Physical and functional interactions between Werner syndrome helicase and mismatch-repair initiation factors. *Nucleic Acids Res* **35:** 5706–5716

Serebrov V, Pyle AM (2004) Periodic cycles of RNA unwinding and pausing by hepatitis C virus NS3 helicase. *Nature* **430:** 476–480

Stauffer ME, Chazin WJ (2004) Physical interaction between replication protein A and Rad51 promotes exchange on single-stranded DNA. *J Biol Chem* **279:** 25638–25645

Sugawara N, Goldfarb T, Studamire B, Alani E, Haber JE (2004) Heteroduplex rejection during single-strand annealing requires Sgs1 helicase and mismatch repair proteins Msh2 and Msh6 but not Pms1. *Proc Natl Acad Sci USA* **101:** 9315–9320

Sun B, Wei K-J, Zhang B, Zhang X-H, Dou S-X, Li M, Xi XG (2008) Impediment of *E. coli* UvrD by DNA-destabilizing force reveals a strained inchworm mechanism of DNA unwinding. *EMBO J* **27:** 3279–3287

Wold MS (1997) Replication protein A: a heterotrimeric, single-stranded DNA-binding protein required for eukaryotic DNA metabolism. *Annu Rev Biochem* **66:** 61–92

Wu L, Hickson ID (2006) DNA helicases required for homologous recombination and repair of damaged replication forks. *Annu Rev Genet* **40:** 279–306

